

RESEARCH ARTICLE

A statistical approach to target detection and localization in the presence of noise

Habib Ammari, Josselin Garnier, and Knut Sølna
 (Received 00 Month 200x; final version received 00 Month 200x)

The problem addressed in this paper is the combined detection and localization of a point reflector embedded in a medium by sensor array imaging when the array response matrix is obtained in a noisy environment. We study a detection test based on reverse-time migration of the array response matrix that is the most powerful for a given false alarm rate and compare it with a test based on the singular values of the response matrix. Moreover, we show that reflector localization should be performed with reverse-time migration rather than any other form of weighted-subspace migration and we give the standard deviation of the localization error.

Keywords: Sensor array imaging, target detection, statistical testing, random matrix theory, extreme value theory.

1. Introduction

The problem addressed in this paper is to detect and localize a point reflector embedded in a medium by probing the medium with time-harmonic scalar waves emitted from and recorded on a sensor array. We use stochastic and statistical tools to study this problem when the array response matrix is acquired in a noisy environment. We consider a clutter noise (small random fluctuations in the background medium) in the multiple scattering regime and/or an additive measurement noise. In both situations, up to a symmetrization of the response matrix, the noise can be modeled by an additive symmetric Gaussian matrix with zero mean [5, 6].

Our first goal is to design an efficient detection procedure. Indeed the known statistical structure of the response matrix allows us to analyze the statistical distribution of the singular values of the matrix in the presence and in the absence of a reflector, and also the statistical behavior of general weighted-subspace migration functionals. The use of random matrix theory [20] and extreme value theory [1] turns out to be convenient. This analysis then allows us to construct detection tests based on the singular values (SV) of the noisy response matrix or based on reverse-time migration that are the most powerful for a given false alarm rate, using the Neyman-Pearson lemma [15]. We show that the migration-based test is more powerful than the SV-based test. We can explain this result by remarking that the migration-based test uses the known structure of the singular vector associated to the point reflector while the SV-based test does not exploit this structure.

Department of Mathematics and Applications, Ecole Normale Supérieure, 45 Rue d'Ulm, 75005 Paris, France (habib.ammari@ens.fr).
 Laboratoire de Probabilités et Modèles Aléatoires & Laboratoire Jacques-Louis Lions, Université Paris VII, 2 Place Jussieu, 75251 Paris Cedex 5, France (garnier@math.jussieu.fr). Corresponding author.
 Department of Mathematics, University of California, Irvine, CA 92697 (ksolna@math.uci.edu).

The second aim of this paper is to provide weighted-subspace migration functionals for localizing the point reflector and to compare their performance. We show the optimality of the reverse-time migration imaging functional in the presence of noise.

The paper is organized as follows. In Sections 3-4 we propose two detection tests, one based on the singular values of the array response matrix and another one based on the reverse-time migration functional of the response matrix. We study general versions of these tests using random matrix theory, in particular recent results on low-rank perturbations of random Gaussian matrices, and extreme value theory for Gaussian fields. We identify the most powerful tests using the Neyman-Pearson lemma and we show that the levels of the tests are prescribed in terms of a Tracy-Widom distribution or a Gumbel distribution. Quantitative calculations allow us to describe the regimes in which the migration-based test is more powerful than the SV-based test. In Section 5 we identify the optimal migration technique for estimating the location of the reflector in the presence of noise by using a Bayesian approach. We find that reverse-time migration is slightly more robust than Kirchhoff migration [9], and that both are much more robust than algorithms of MUSIC-type (which stands for MULTiple SIGNAL Classification) [10, 16, 19, 24]. We compute the standard deviation of the error in the localization for the optimal reverse-time migration technique.

2. Problem formulation

2.1. The response matrix

Let us consider the propagation of scalar waves in a three-dimensional medium. In the presence of a localized reflector and small random fluctuations of the medium (clutter noise), the speed of propagation can be modeled by

$$\frac{1}{c^2(\mathbf{x})} = \frac{1}{c_0^2} (1 + \sigma_{\text{clu}} V_{\text{clu}}(\mathbf{x}) + \sigma_{\text{r}} V_{\text{ref}}(\mathbf{x})). \quad (1)$$

Here

- the constant c_0 is the known background speed,
- the random process $V_{\text{clu}}(\mathbf{x})$ represents the cluttered medium,
- the local variation $V_{\text{ref}}(\mathbf{x})$ of the speed of propagation induced by the reflector at \mathbf{x}_{ref} is

$$V_{\text{ref}}(\mathbf{x}) = \mathbf{1}_{\Omega_{\text{ref}}}(\mathbf{x} - \mathbf{x}_{\text{ref}}), \quad (2)$$

where Ω_{ref} is a compactly supported domain with volume l_{ref}^3 .

Suppose that a time-harmonic point source acts at the point $\mathbf{y} \in \mathbb{R}^3$ with frequency ω . The field in the presence of the reflector and clutter noise is the solution $\hat{u}(\cdot, \mathbf{y})$ to the following transmission problem:

$$\Delta_{\mathbf{x}} \hat{u} + \frac{\omega^2}{c^2(\mathbf{x})} \hat{u} = -\delta_{\mathbf{y}}(\mathbf{x}), \quad (3)$$

with the radiation condition imposed on \hat{u} .

Suppose that we have co-localized transmitter and receiver arrays $\{\mathbf{y}_1, \dots, \mathbf{y}_n\}$ of n elements, used to detect the reflector. The response matrix $\mathbf{A} = (A_{jl})_{j,l=1,\dots,n}$ describes the transmit-receive process performed at this array. In the presence of a

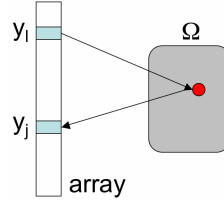


Figure 1. Sensor array imaging for the detection and localization of a reflector buried in a search region Ω .

reflector and clutter noise the field received by the j th receiving element \mathbf{y}_j when the wave is emitted from \mathbf{y}_l is $\hat{u}(\mathbf{y}_j, \mathbf{y}_l)$ (Figure 1). If we remove the incident field then it is $\hat{u}(\mathbf{y}_j, \mathbf{y}_l) - \hat{G}_0(\omega, \mathbf{y}_j, \mathbf{y}_l)$. The incident field is the homogeneous Green function $\hat{G}_0(\omega, \mathbf{x}, \mathbf{y})$ given by

$$\hat{G}_0(\omega, \mathbf{x}, \mathbf{y}) = \frac{e^{i\frac{\omega}{c_0}|\mathbf{x}-\mathbf{y}|}}{4\pi|\mathbf{x}-\mathbf{y}|}. \quad (4)$$

Finally, taking into account measurement noise, the entries of the response matrix are

$$A_{jl} = \hat{u}(\mathbf{y}_j, \mathbf{y}_l) - \hat{G}_0(\omega, \mathbf{y}_j, \mathbf{y}_l) + w_{jl}, \quad (5)$$

where w_{jl} represents the additive measurement noise. By reciprocity the response matrix is complex symmetric in the absence of measurement noise.

2.2. The response matrix in the presence of a reflector and in the absence of noise

In the Born approximation (see Appendix A) and in the absence of measurement or clutter noise the response matrix \mathbf{A}_0 has the form

$$A_{0jl} = \frac{\omega^2}{c_0^2} \sigma_r l_{\text{ref}}^3 \hat{G}_0(\omega, \mathbf{y}_j, \mathbf{x}_{\text{ref}}) \hat{G}_0(\omega, \mathbf{x}_{\text{ref}}, \mathbf{y}_l), \quad j, l = 1, \dots, n,$$

where σ_r is the scattering amplitude and l_{ref}^3 is the volume of the scatterer. We introduce the normalized vector of Green's functions from the sensor array to the point \mathbf{x} , the so called illumination vector:

$$\mathbf{g}(\mathbf{x}) := \frac{1}{\left(\sum_{l=1}^n |\hat{G}_0(\omega, \mathbf{x}, \mathbf{x}_l)|^2\right)^{1/2}} \left(\hat{G}_0(\omega, \mathbf{x}, \mathbf{x}_j)\right)_{j=1, \dots, n}. \quad (6)$$

We can then write the response matrix in the form

$$\mathbf{A}_0 = \sigma_{\text{ref}} \mathbf{g}(\mathbf{x}_{\text{ref}}) \mathbf{g}(\mathbf{x}_{\text{ref}})^T, \quad (7)$$

with

$$\sigma_{\text{ref}} := \frac{\omega^2}{c_0^2} \sigma_r l_{\text{ref}}^3 \left(\sum_{l=1}^n |\hat{G}_0(\omega, \mathbf{x}_{\text{ref}}, \mathbf{x}_l)|^2 \right). \quad (8)$$

Here T denotes the transpose. The matrix \mathbf{A}_0 has rank 1 and its unique non-zero singular value is σ_{ref} . Note that σ_{ref} scales as n . If the sensor array is at distance L from the reflector, and if the diameter of the sensor array is small compared to L , then

$$\sigma_{\text{ref}} \simeq \frac{\omega^2 \sigma_{\text{r}} l_{\text{ref}}^3}{16\pi^2 c_0^2 L^2} n = \frac{\sigma_{\text{r}} l_{\text{ref}}^3}{4\lambda_0^2 L^2} n, \quad (9)$$

where $\lambda_0 = 2\pi c_0/\omega$ is the wavelength.

2.3. The response matrix in the absence of a reflector and in the presence of noise

In the case of clutter noise in the multiple scattering regime, the response matrix \mathbf{A} is complex symmetric with Gaussian statistics. The matrix satisfies $A_{jl} = A_{lj}$ and the entries A_{jl} , $j \leq l$ are independent complex Gaussian random variables with mean zero and variance δ^2 off the diagonal ($j \neq l$) and $2\delta^2$ on the diagonal $j = l$. Here we have taken into account the enhanced backscattering effect [5, 6].

In the case of measurement noise, the response matrix \mathbf{A} is complex with Gaussian statistics. The entries A_{jl} , $j, l = 1, \dots, n$, are independent complex Gaussian random variables with mean zero and variance $2\delta^2$. Since we know that the unperturbed response matrix in the presence of a reflector is symmetric by reciprocity, we symmetrize the measured response matrix and introduce $\mathbf{A}^s := (\mathbf{A} + \mathbf{A}^T)/2$. The matrix satisfies $A_{jl}^s = A_{lj}^s$ and the entries A_{jl}^s , $j \leq l$ are independent complex Gaussian random variables with mean zero and variance δ^2 off the diagonal ($j \neq l$) and $2\delta^2$ on the diagonal $j = l$.

In both situations the response matrix in the absence of a reflector is of the form

$$\mathbf{A} = \delta \mathbf{W}, \quad (10)$$

where \mathbf{W} is a complex symmetric Gaussian matrix with zero mean and with variance equal to one off the diagonal and to two on the diagonal.

2.4. The response matrix in the presence of a reflector and in the presence of noise

The interesting problem is the case in which there is a point reflector and noise. We consider the situation in which there is clutter noise in the multiple scattering regime, or the situation in which there is an additive measurement noise and the response matrix is symmetrized. In both situations the response matrix \mathbf{A} can be modeled by [6]:

$$\mathbf{A} = \mathbf{A}_0 + \delta \mathbf{W}, \quad (11)$$

where \mathbf{A}_0 is given by (7) and \mathbf{W} is a complex symmetric Gaussian matrix with zero mean and with variance equal to one off the diagonal and to two on the diagonal. In the presence of clutter noise one should use the coherent (or average) Green's function in the matrix \mathbf{A}_0 defined by (7) instead of the homogeneous Green's function. This means that we should incorporate a damping $\gamma(\omega)$ in the Green's function [2]:

$$\hat{G}(\omega, \mathbf{x}, \mathbf{y}) = \hat{G}_0(\omega, \mathbf{x}, \mathbf{y}) \exp(-\gamma(\omega)|\mathbf{x} - \mathbf{y}|).$$

The problem we consider is to detect and localize the reflector from the response matrix \mathbf{A} in such a situation.

3. Detection of a point reflector by Singular Value Decomposition

The idea that it is possible to construct a detection test that predicts the presence of a target when the largest singular value of the response matrix exceeds some threshold value is described and analyzed in [6]. In this section we carry out a complete statistical analysis and we give in Proposition 3.3 the statistical distribution of the ratio of the largest singular value over the l^2 -norm of the $(n-1)$ other singular values of the noisy response matrix in the absence and in the presence of a reflector. This allows us to calibrate the false alarm rate of the optimal SV-based detection test based on Neyman-Pearson theory and to compute the probability of detection of the test.

3.1. Singular Value Decomposition of the response matrix in the absence of a reflector and in the presence of noise

We consider here the situation in which there is clutter noise in the multiple scattering regime, or the situation in which there is an additive measurement noise and the response matrix is symmetrized. In both situations the response matrix \mathbf{A} is of the form (10). We denote by $\sigma_1^{(n)} \geq \sigma_2^{(n)} \geq \sigma_3^{(n)} \geq \dots \geq \sigma_n^{(n)}$ the singular values of the response matrix \mathbf{A} sorted by decreasing order and by $N^{(n)}$ the corresponding integrated density of states defined by

$$N^{(n)}([a, b]) := \frac{1}{n} \text{Card} \left\{ l = 1, \dots, n, \sigma_l^{(n)} \in [a, b] \right\}, \text{ for any } a < b.$$

$N^{(n)}$ is a counting measure which consists of a sum of Dirac masses:

$$N^{(n)} = \frac{1}{n} \sum_{j=1}^n \delta_{\sigma_j^{(n)}}.$$

We introduce the parameter $\sigma_c = \sqrt{n}\delta$. For large n we have the following results.

Proposition 3.1:

- a) *The random measure $N^{(n)}$ almost surely converges to the deterministic absolutely continuous measure N with compact support:*

$$N([\sigma_u, \sigma_v]) = \int_{\sigma_u}^{\sigma_v} \rho(\sigma) d\sigma, \quad \rho(\sigma) = \frac{1}{\sigma_c} \rho_{\text{qc}}\left(\frac{\sigma}{\sigma_c}\right), \quad (12)$$

where ρ_{qc} is the quarter-circle law given by

$$\rho_{\text{qc}}(\sigma) = \begin{cases} \frac{1}{\pi} \sqrt{4 - \sigma^2} & \text{if } 0 < \sigma \leq 2, \\ 0 & \text{otherwise.} \end{cases} \quad (13)$$

- b) *The normalized l^2 -norm of the singular values satisfies*

$$n \left[\frac{1}{n} \sum_{j=1}^n (\sigma_j^{(n)})^2 - \sigma_c^2 \right] \xrightarrow{n \rightarrow \infty} \sigma_c^2 + \sqrt{2} \sigma_c^2 Z \text{ in distribution,} \quad (14)$$

where Z follows a Gaussian distribution with mean zero and variance one.

Here, the function ρ is the asymptotic density of states and $\rho(\sigma)d\sigma$ gives the proportion of singular values of the response matrix that lie in the elementary interval $[\sigma, \sigma + d\sigma]$.

Proof. Point a) is classical [21] and was already noticed in [6]. Point b) follows from the expression of the normalized l^2 -norm of the singular values in terms of the entries of the matrix:

$$\frac{1}{n} \sum_{j=1}^n (\sigma_j^{(n)})^2 = \frac{1}{n} \text{Tr}(\mathbf{A}^T \mathbf{A}) = \frac{1}{n} \sum_{j=1}^n |A_{jj}|^2 + \frac{2}{n} \sum_{j < l} |A_{jl}|^2,$$

and from the application of the central limit theorem in the regime $n \gg 1$. □

3.2. Singular Value Decomposition of the response matrix in the presence of a reflector and in the presence of noise

Here we consider the response matrix \mathbf{A} obtained with a reflector in the presence of noise. It is modeled by (11). Let us denote by $\sigma_1^{(n)} \geq \sigma_2^{(n)} \geq \sigma_3^{(n)} \geq \dots \geq \sigma_n^{(n)}$ the singular values of the matrix \mathbf{A} . We introduce as above the parameter $\sigma_c = \sqrt{n}\delta$. For large n , we can expand the distribution of the singular values and we get the following results:

Proposition 3.2:

- a) If $\sigma_c > \sigma_{\text{ref}}$, then the largest singular value $\sigma_1^{(n)}$ obeys a non-Gaussian statistics. More specifically, it is equal to $2\sigma_c$ up to a random correction of order $\sigma_c n^{-2/3}$:

$$\sigma_1^{(n)} \stackrel{\text{dist.}}{=} \sigma_c [2 + 2^{-2/3} n^{-2/3} Z_1 + o(n^{-2/3})],$$

where $\stackrel{\text{dist.}}{=}$ means “equal in distribution” and the random variable Z_1 follows a Tracy-Widom distribution of type 1:

$$\mathbb{P}(Z_1 \leq z) = \int_{-\infty}^z p_{\text{TW1}}(x) dx = \exp\left(-\frac{1}{2} \int_z^{\infty} \varphi(x) + (x-z)\varphi^2(x) dx\right),$$

$$\mathbb{E}[Z_1] \simeq -1.21, \quad \text{Var}(Z_1) \simeq 1.61.$$

Here \mathbb{E} stands for the expectation (mean value), Var for the variance, and φ is the solution of the Painlevé equation

$$\varphi''(x) = x\varphi(x) + 2\varphi(x)^3, \quad \varphi(x) \stackrel{x \rightarrow +\infty}{\simeq} \text{Ai}(x), \tag{15}$$

Ai being the Airy function.

- b) If $\sigma_c < \sigma_{\text{ref}}$, then the largest singular value $\sigma_1^{(n)}$ obeys Gaussian statistics with the mean and variance

$$\mathbb{E}[\sigma_1^{(n)}] = \sigma_{\text{ref}} + \sigma_c^2 \sigma_{\text{ref}}^{-1}, \quad \text{Var}(\sigma_1^{(n)}) = \frac{1}{n} \sigma_c^2 (1 - \sigma_c^2 \sigma_{\text{ref}}^{-2}). \tag{16}$$

- c) For any σ_c and σ_{ref} , the second singular value $\sigma_2^{(n)}$ is equal to $2\sigma_c$ to leading order as $n \rightarrow \infty$.

d) For any σ_c and σ_{ref} , the normalized l^2 -norm of the $n-1$ smallest singular values satisfies

$$n^p \left[\frac{1}{n-1} \sum_{j=2}^n (\sigma_j^{(n)})^2 - \sigma_c^2 \right] \xrightarrow{n \rightarrow \infty} 0 \text{ in probability,} \quad (17)$$

for any $p \in (0, 1)$.

We stress here that Eq. (16) is not an expansion valid only for $\sigma_c \ll \sigma_{\text{ref}}$, it is valid for any $\sigma_c < \sigma_{\text{ref}}$ (see Figure 2). Point a) was already noticed in [6] in the case $\sigma_{\text{ref}} = 0$. Point d) shows that the fluctuations of the normalized l^2 -norm of the $n-1$ smallest singular values are smaller than the fluctuations of the largest singular value which are of order $n^{-2/3}$ or $n^{-1/2}$ by a) and b).

Proof. Points a) and b) are proved in [17]. Point c) is proved in [13]. In order to prove point d) we first note that we have

$$\frac{1}{n-1} \sum_{j=2}^n (\sigma_j^{(n)})^2 = \frac{1}{n-1} \sum_{j=1}^n (\sigma_j^{(n)})^2 - \frac{(\sigma_1^{(n)})^2}{n-1} = \frac{1}{n-1} \text{Tr}(\overline{\mathbf{A}}^T \mathbf{A}) - \frac{(\sigma_1^{(n)})^2}{n-1}.$$

We can write

$$n \left[\frac{1}{n-1} \sum_{j=2}^n (\sigma_j^{(n)})^2 - \sigma_c^2 \right] = \frac{n^2}{n-1} \left[\frac{1}{n} \text{Tr}(\overline{\mathbf{A}}^T \mathbf{A}) - \frac{\sigma_{\text{ref}}^2}{n} - \sigma_c^2 \right] - \frac{n}{n-1} \left[(\sigma_1^{(n)})^2 - \sigma_{\text{ref}}^2 - \sigma_c^2 \right].$$

The second term converges in probability to $\bar{\sigma}_1^2 - \sigma_{\text{ref}}^2 - \sigma_c^2$, where we have denoted by $\bar{\sigma}_1 = 2\sigma_c$ if $\sigma_c > \sigma_{\text{ref}}$ and $= \sigma_{\text{ref}} + \sigma_c^2 \sigma_{\text{ref}}^{-1}$ if $\sigma_c < \sigma_{\text{ref}}$ the deterministic leading order term of $\sigma_1^{(n)}$. The first term converges in distribution by the central limit theorem:

$$n \left[\frac{1}{n} \text{Tr}(\overline{\mathbf{A}}^T \mathbf{A}) - \frac{\sigma_{\text{ref}}^2}{n} - \sigma_c^2 \right] \xrightarrow{n \rightarrow \infty} \sigma_c^2 + \sqrt{2} \sigma_c^2 Z \text{ in distribution,}$$

where Z follows a Gaussian distribution with mean zero and variance one. Therefore, by Slutsky's theorem [18],

$$n \left[\frac{1}{n-1} \sum_{j=2}^n (\sigma_j^{(n)})^2 - \sigma_c^2 \right] \xrightarrow{n \rightarrow \infty} 2\sigma_c^2 + \sigma_{\text{ref}}^2 - \bar{\sigma}_1^2 + \sqrt{2} \sigma_c^2 Z \text{ in distribution,} \quad (18)$$

which gives the result by Markov inequality [25]. \square

Several interesting features can be noted:

1) The noise generates small singular values, whose largest one is $\sigma_2^{(n)}$ which is of the order of $2\sigma_c = 2\delta\sqrt{n}$.

2) The first singular value, $\sigma_1^{(n)}$, corresponding to the reflector, increases as the noise increases. This is a manifestation of the level repulsion phenomenon well known in random matrix theory [20]: the small singular values (and in particular $\sigma_2^{(n)}$) increase as the noise level increases, and the first singular value is repelled (see Figure 2).

3) The first singular value, corresponding to the reflector, and the second singular value, that is the largest singular value generated by the noise, are well separated as long as $2\sigma_c < \sigma_{\text{ref}}$, i.e. $2\delta\sqrt{n} < \sigma_{\text{ref}}$. This indicates, as we will see in more detail

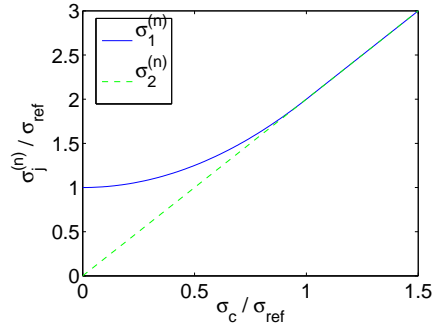


Figure 2. First and second singular values as a function of the noise level $\sigma_c/\sigma_{\text{ref}}$. Here we plot the expected values, and the standard deviations are small (of order $n^{-2/3}$ or $n^{-1/2}$ as described in Proposition 3.2).

below, that it is possible to detect the reflector based on the singular values as long as $2\delta\sqrt{n} < \sigma_{\text{ref}}$.

3.3. SV-based detection test

Let us consider the ratio of the first singular value over the L^2 -norm of the other singular values

$$R := \frac{\sigma_1^{(n)}}{\left(\frac{1}{n-1} \sum_{j=2}^n (\sigma_j^{(n)})^2\right)^{1/2}}. \quad (19)$$

The statistical distribution of the ratio R , in the presence and in the absence of a reflector, is given by the following proposition.

Proposition 3.3: *In the asymptotic regime $n \gg 1$, we have:*

- (1) *If the response matrix is obtained without a reflector, then the ratio (19) has the following statistical distribution:*

$$R \stackrel{\text{dist.}}{=} 2 + \frac{1}{2^{2/3}n^{2/3}}Z_1, \quad (20)$$

where Z_1 is a random variable following a Tracy-Widom distribution of type 1.

- (2) *If the response matrix is obtained with a reflector, then:*
 - a) *For $\sigma_c < \sigma_{\text{ref}}$, the ratio (19) has the following statistical distribution*

$$R \stackrel{\text{dist.}}{=} \frac{\sigma_{\text{ref}}}{\sigma_c} + \frac{\sigma_c}{\sigma_{\text{ref}}} + \frac{1}{\sqrt{2n}}\sqrt{1 - \sigma_c^2\sigma_{\text{ref}}^{-2}}Z, \quad (21)$$

where Z follows a Gaussian distribution with mean zero and variance one.

- b) *For $\sigma_c > \sigma_{\text{ref}}$ we have (20).*

Proof. For point (i):

$$\begin{aligned} (2n)^{2/3}(R - 2) &= (2n)^{2/3} \left(\frac{\sigma_1^{(n)}}{\left(\frac{1}{n-1} \sum_{j=2}^n (\sigma_j^{(n)})^2\right)^{1/2}} - 2 \right) \\ &= (2n)^{2/3} \frac{\sigma_1^{(n)} - 2\sigma_c}{\sigma_c} + \sigma_1^{(n)}(2n)^{2/3} \left(\frac{1}{\left(\frac{1}{n-1} \sum_{j=2}^n (\sigma_j^{(n)})^2\right)^{1/2}} - \frac{1}{\sigma_c} \right). \end{aligned}$$

By Proposition 3.2 the first term of the right-hand side converges in distribution to Z_1 and the second term converges in probability to 0. Using again Slutsky's theorem we obtain the result. Point (ii) can be shown in the same way. \square

Based on the previous proposition and the Neyman-Pearson lemma, it is possible to design an optimal test based on the singular values of the response matrix for the detection of a reflector.

Define H_0 the (null) hypothesis to be tested and H_A the (alternative) hypothesis:

- H_0 : there is no reflector,
- H_A : there is a reflector.

We want to test H_0 against H_A . Two types of errors can be made:

- Type I errors correspond to rejecting H_0 when it is correct: *false alarm*. The probability of type I error (false alarm rate) is

$$\alpha := \mathbb{P}(\text{accept } H_A | H_0 \text{ true}),$$

- Type II errors correspond to accepting H_0 when it is false: *missed detection*. The probability of type II error (probability of missed detection) is

$$\beta := \mathbb{P}(\text{accept } H_0 | H_A \text{ true}).$$

The probability of detection (power of the test) is therefore given by $1 - \beta$. The general result is that it is not possible to maximize the probability of detection and minimize the false alarm rate at the same time. However, amongst all possible tests with a given false alarm rate, it is possible to identify the best test that maximizes the probability of detection. Given the data, the decision rule for accepting H_0 or not can be derived accordingly from the Neyman-Pearson lemma:

Neyman-Pearson lemma: *Let Y be the set of all possible data and let $f_0(y)$ and $f_1(y)$ be the probability densities of Y under the null and alternative hypotheses:*

$$\mathbb{P}(Y \in A | H_0 \text{ true}) = \int_A f_0(y) dy, \quad \mathbb{P}(Y \in A | H_0 \text{ false}) = \int_A f_1(y) dy.$$

The most powerful test has a critical region defined by

$$\mathcal{Y}_\alpha := \left\{ y \in Y \mid \frac{f_1(y)}{f_0(y)} \geq \eta_\alpha \right\},$$

for a threshold η_α satisfying

$$\int_{y \in \mathcal{Y}_\alpha} f_0(y) dy = \alpha.$$

Neyman-Pearson test: *If the data is y , we reject H_0 if the likelihood ratio $\frac{f_1(y)}{f_0(y)} > \eta_\alpha$ and accept H_0 otherwise. The power of the (most powerful) test is given by*

$$1 - \beta = \int_{y \in \mathcal{Y}_\alpha} f_1(y) dy.$$

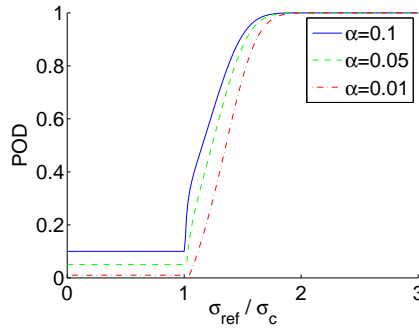


Figure 3. Probability of detection of the SV-based test as a function of the signal-to-noise ratio $\sigma_{\text{ref}}/\sigma_c$, for different false alarm rates α .

If the data (i.e. the measured response matrix) gives the ratio R , then we propose to use a test of the form $R > r$ for the alarm corresponding to the presence of a reflector. By the Neyman-Pearson lemma the decision rule of accepting H_A if and only if $R > r_\alpha$ maximizes the probability of detection (POD) for a given false alarm rate (FAR) α

$$\text{FAR} = \alpha = \mathbb{P}(R > r_\alpha | H_0),$$

with the threshold

$$r_\alpha = 2 + \frac{1}{2^{2/3} n^{2/3}} \Phi_{\text{TW}_1}^{-1}(1 - \alpha), \quad (22)$$

where Φ_{TW_1} is the cumulative distribution function of the Tracy-Widom distribution of type 1. The computation of the threshold r_α is easy since it depends only on the number of sensors n and on the false alarm probability α . This test is therefore universal. Note that we should use a Tracy-Widom distribution table, and not a Gaussian table. We have, for instance, $\Phi_{\text{TW}_1}^{-1}(0.9) \simeq 0.45$, $\Phi_{\text{TW}_1}^{-1}(0.95) \simeq 0.98$ and $\Phi_{\text{TW}_1}^{-1}(0.99) \simeq 2.02$.

Remark: In principle the decision region of the Neyman-Pearson test could be two-sided since the Gaussian distribution has a heavier left tail $\sim \exp(-z^2/2)$ than the Tracy-Widom distribution $\sim \exp(-|z|^3/24)$ as $z \rightarrow -\infty$ [8], but this is not important in practice because the left side is negligible compared to the right side in our framework.

The probability of detection $1 - \beta$ is the probability to sound the alarm when there is a reflector:

$$\text{POD} = 1 - \beta = \mathbb{P}(R > r_\alpha | H_A).$$

It depends on the value σ_{ref} and on the noise level $\sigma_c = \sqrt{n}\delta$. Here we find that the probability of detection is

$$\text{POD} = 1 - \beta = \Phi\left(\sqrt{2n} \frac{\frac{\sigma_{\text{ref}}}{\sigma_c} + \frac{\sigma_c}{\sigma_{\text{ref}}} - r_\alpha}{\sqrt{1 - (\sigma_c/\sigma_{\text{ref}})^2}}\right),$$

where Φ is the cumulative distribution function of the normal distribution with

mean zero and variance one. We have for large n

$$\text{POD} \simeq 1 - \frac{e^{-n\sigma_{\text{ref},c}^2}}{\sqrt{4\pi n\sigma_{\text{ref},c}^2}}, \quad \text{where } \sigma_{\text{ref},c} = \frac{\frac{\sigma_{\text{ref}}}{\sigma_c} + \frac{\sigma_c}{\sigma_{\text{ref}}} - 2}{\sqrt{1 - (\sigma_c/\sigma_{\text{ref}})^2}},$$

so that the theoretical test performance improves very rapidly with n once $\sigma_{\text{ref}} > \sigma_c$. This result is indeed valid as long as $\sigma_{\text{ref}} > \sigma_c$. When $\sigma_{\text{ref}} < \sigma_c$, so that the reflector is ‘‘hidden in noise’’ (more exactly, the singular value corresponding to the reflector is buried into the quarter-circle distribution of the other singular values), then we have $1 - \beta = 1 - \Phi_{\text{TW1}}(\Phi_{\text{TW1}}^{-1}(1 - \alpha)) = \alpha$. Therefore the probability of detection is given by

$$\text{POD} = \max \left\{ \Phi \left(\sqrt{n} \frac{\frac{\sigma_{\text{ref}}}{\sigma_c} + \frac{\sigma_c}{\sigma_{\text{ref}}} - r_\alpha}{\sqrt{1 - (\sigma_c/\sigma_{\text{ref}})^2}}, \alpha \right), \alpha \right\}. \quad (23)$$

To summarize, the SV-based test becomes efficient (i.e., powerful) when $\sigma_{\text{ref}} > \sigma_c$. Since σ_{ref} scales as n while $\sigma_c = \sqrt{n}\delta$, the SV-based test becomes more and more powerful as the number n of sensors increases and the variance δ^2 of the entries of the response matrix decreases.

4. Detection of a point reflector by migration

In the presence of a point reflector at \mathbf{x}_{ref} and in the presence of noise the response matrix is of the form (11). In the previous section we studied a SV-based test that uses optimally the singular values of the response matrix. Here we would like to exploit the known structure of the main singular vector of the unperturbed response matrix and to design a better detection test using this information. For this we can consider a general class of weighted-subspace migration functionals. As we will see in Section 5, the optimal weighted-subspace migration functional in the presence of additive noise is the reverse-time imaging functional defined by

$$\mathcal{I}_{\text{RT}}(\mathbf{x}) := \overline{\mathbf{g}(\mathbf{x})}^T \mathbf{A} \mathbf{g}(\mathbf{x}), \quad (24)$$

where $\mathbf{g}(\mathbf{x})$ is the normalized vector of Green’s functions (6). Accordingly, we can design an optimal test based on the maximal value of the reverse-time imaging functional reached in the search region. Such a detection test was proposed and implemented in [7]. In this section we carry out a complete statistical analysis of the test and we clarify under which conditions the migration-based test is more powerful than the SV-based test. The strategy for the analysis is similar as in the previous section. We first compute the statistical distribution of the reverse-time imaging functional in the absence and in the presence of a reflector, and then we obtain the most powerful test by the Neyman-Pearson lemma.

4.1. The imaging functional in the presence of a reflector and in the absence of noise

In the absence of noise $\delta = 0$ the response matrix has the form (7) and the imaging functional is given by

$$\mathcal{I}_{\text{RT}}(\mathbf{x}) = \mathcal{I}_0(\mathbf{x}) := \sigma_{\text{ref}} \mathcal{H}(\mathbf{x}, \mathbf{x}_{\text{ref}})^2, \quad \mathcal{H}(\mathbf{x}, \mathbf{y}) := \overline{\mathbf{g}(\mathbf{x})}^T \mathbf{g}(\mathbf{y}), \quad (25)$$

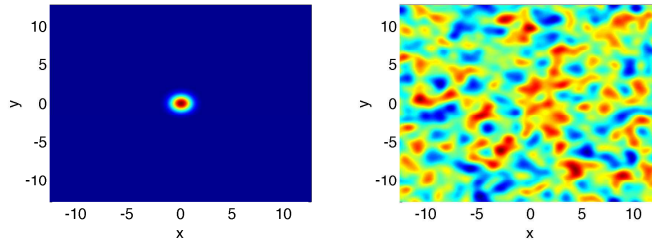


Figure 4. Left: Point spread function corresponding to the imaging functional \mathcal{I}_{RT} in the presence of a reflector at $\mathbf{x}_{\text{ref}} = \mathbf{0}$ and in the absence of noise. Right: Speckle pattern corresponding to the imaging functional in the absence of a reflector and in the presence of noise. Here the function $h(\mathbf{x}) = \exp(-|\mathbf{x}|^2)$.

where σ_{ref} is given by (8). The function \mathcal{H} has been studied extensively in imaging, it is the point spread function that describes the spatial profile of the peak obtained at the reflector location in the imaging functional when the reflector is point-like (Figure 4, left). A general result obtained by Cauchy-Schwarz inequality is that the maximum of $\mathcal{H}(\mathbf{x}, \mathbf{y})$ is reached at $\mathbf{x} = \mathbf{y}$ and it is equal to one. Therefore, the maximum of \mathcal{I}_0 over a search domain Ω (that contains \mathbf{x}_{ref}) is reached at $\mathbf{x} = \mathbf{x}_{\text{ref}}$ and it is equal to

$$\max_{\mathbf{x} \in \Omega} |\mathcal{I}_0(\mathbf{x})|^2 = \sigma_{\text{ref}}^2. \quad (26)$$

Full aperture array. If the sensor array is dense (i.e. the intersensor distance is smaller than half a wavelength) and completely surrounds the region of interest, then Helmholtz-Kirchhoff theorem states that $\mathcal{H}(\mathbf{x}, \mathbf{y})$ is proportional to the imaginary part of the Green function $\hat{G}(\omega, \mathbf{x}, \mathbf{y})$. If the medium is homogeneous and three-dimensional, then we find

$$\mathcal{I}_0(\mathbf{x}) = \sigma_{\text{ref}} h(\mathbf{x} - \mathbf{x}_{\text{ref}}), \text{ where } h(\mathbf{x}) = \text{sinc}^2\left(\frac{2\pi|\mathbf{x}|}{\lambda_0}\right).$$

Finite aperture array. If the medium is homogeneous and three-dimensional, if the sensor array is dense and occupies the domain $D_a \times \{0\}$, with $D_a \subset \mathbb{R}^2$ with diameter a , and the search region is a domain Ω around $(0, 0, L)$, then in the regime $a \ll L$ and $\lambda_0 L \ll a^2$ we have

$$\mathcal{I}_0(\mathbf{x}) = \sigma_{\text{ref}} h(\mathbf{x} - \mathbf{x}_{\text{ref}}),$$

where, for $\mathbf{x} = (\mathbf{x}_{\perp}, x_3)$,

$$h(\mathbf{x}) = \frac{1}{|D_a|^2} \left(e^{-i\frac{2\pi}{\lambda_0}x_3} \int_{D_a} \exp\left(i\frac{2\pi\mathbf{y}_{\perp}}{\lambda_0 L} \cdot \mathbf{x}_{\perp} + i\frac{\pi|\mathbf{y}_{\perp}|^2}{\lambda_0 L^2}x_3\right) d\mathbf{y}_{\perp} \right)^2, \quad (27)$$

which shows that the width of the function $|h(\mathbf{x})|$ is of the order of $\lambda_0 L/a$ in the transverse directions (\mathbf{x}_{\perp}) and $\lambda_0 L^2/a^2$ in the longitudinal direction (x_3). These are the classical Rayleigh resolution formulas [12].

4.2. The imaging functional in the absence of a reflector and in the presence of noise

In the absence of a reflector and in the presence of noise the imaging functional is a complex Gaussian random field (Figure 4, right). Its mean is zero and, taking into

account the covariance function of the response matrix, the covariance function of the imaging functional is:

$$\mathbb{E}[\mathcal{I}_{\text{RT}}(\mathbf{x})\mathcal{I}_{\text{RT}}(\mathbf{y})] = 0, \quad \mathbb{E}[\mathcal{I}_{\text{RT}}(\mathbf{x})\overline{\mathcal{I}_{\text{RT}}(\mathbf{y})}] = 2\delta^2\mathcal{H}(\mathbf{x}, \mathbf{y})^2. \quad (28)$$

Full aperture array. In the case in which the medium is homogeneous and three-dimensional with background speed c_0 and the array completely surrounds the region of interest, \mathcal{I}_{RT} is a stationary Gaussian random field with mean zero, variance $2\delta^2$, and covariance function:

$$\mathbb{E}[\mathcal{I}_{\text{RT}}(\mathbf{x})\overline{\mathcal{I}_{\text{RT}}(\mathbf{y})}] = 2\delta^2h(\mathbf{x} - \mathbf{y}), \quad h(\mathbf{x}) = \text{sinc}^2\left(\frac{2\pi|\mathbf{x}|}{\lambda_0}\right).$$

The random field is a speckle pattern whose hotspot profiles are close to the function h . Here the hotspot profile refers to the local shape of the field around a local maximum (see Appendix B). The hotspot volume is defined as

$$V_c := \frac{\pi^{3/2}}{(\det \mathbf{H})^{1/2}}, \quad \mathbf{H} := (-\partial_{x_j x_l}^2 h(\mathbf{0}))_{j,l=1,\dots,3}.$$

Here the matrix \mathbf{H} is proportional to the identity and we have

$$-\partial_{x_j x_j}^2 h(\mathbf{0}) = \frac{8\pi^2}{3\lambda_0^2}, \quad j = 1, \dots, 3, \quad V_c = \frac{3^{3/2}\lambda_0^3}{2^{9/2}\pi^{3/2}}.$$

The maximum of the functional over a domain Ω whose volume is much larger than the hotspot volume is (see Appendix B)

$$\max_{\mathbf{x} \in \Omega} |\mathcal{I}_{\text{RT}}(\mathbf{x})|^2 = 2\delta^2 \left(\ln \frac{|\Omega|}{V_c} + \frac{3}{2} \ln \ln \frac{|\Omega|}{V_c} - \ln Z_0 \right), \quad (29)$$

where Z_0 follows an exponential distribution with mean one, or equivalently, $-\ln Z_0$ follows a Gumbel distribution.

Finite aperture array. In the case in which the medium is homogeneous and three-dimensional with background speed c_0 , the sensor array is dense and occupies the domain $D_a \times \{0\}$, with $D_a \subset \mathbb{R}^2$ with diameter a , and the search region is a domain Ω around $(0, 0, L)$, then the field \mathcal{I}_{RT} is a stationary Gaussian random field with mean zero, variance $2\delta^2$, and covariance function:

$$\mathbb{E}[\mathcal{I}_{\text{RT}}(\mathbf{x})\overline{\mathcal{I}_{\text{RT}}(\mathbf{y})}] = 2\delta^2h(\mathbf{x} - \mathbf{y}),$$

where h is given by (27). Here h is complex valued $h(\mathbf{x}) = h_r(\mathbf{x}) + ih_i(\mathbf{x})$ where h_r is even and h_i is odd. We denote $\nabla h_i(\mathbf{0}) = i\mathbf{h}_1$ and introduce the auxiliary field $\mathcal{I}_a(\mathbf{x}) = \mathcal{I}_{\text{RT}}(\mathbf{x}) \exp(-i\mathbf{h}_1 \cdot \mathbf{x})$. The Gaussian field \mathcal{I}_a has the same intensity as \mathcal{I}_{RT} and it is easier to get the results with this auxiliary field, which is such that $\mathbb{E}[\mathcal{I}_a(\mathbf{x})\overline{\mathcal{I}_a(\mathbf{x})}] = 0$, $\mathbb{E}[\mathcal{I}_a(\mathbf{x})\nabla\overline{\mathcal{I}_a(\mathbf{x})}] = \mathbf{0}$, and $\mathbb{E}[\nabla\mathcal{I}_a(\mathbf{x})\nabla\overline{\mathcal{I}_a(\mathbf{x})}^T] = -\mathbf{H}$, where the matrix \mathbf{H} is given by

$$\mathbf{H} = (-\partial_{x_j x_l}^2 h_r(\mathbf{0}) - \partial_{x_j} h_i(\mathbf{0})\partial_{x_l} h_i(\mathbf{0}))_{j,l=1,\dots,3}$$

which reads explicitly as ($j, l = 1, 2$)

$$\begin{aligned} H_{jl} &= \frac{8\pi^2}{\lambda_0^2 L^2} \left[\frac{1}{|D_a|} \int_{D_a} y_j y_l d\mathbf{y}_\perp - \left(\frac{1}{|D_a|} \int_{D_a} y_j d\mathbf{y}_\perp \right) \left(\frac{1}{|D_a|} \int_{D_a} y_l d\mathbf{y}_\perp \right) \right], \\ H_{j3} &= \frac{4\pi^2}{\lambda_0^2 L^3} \left[\frac{1}{|D_a|} \int_{D_a} y_j |\mathbf{y}_\perp|^2 d\mathbf{y}_\perp - \left(\frac{1}{|D_a|} \int_{D_a} y_j d\mathbf{y}_\perp \right) \left(\frac{1}{|D_a|} \int_{D_a} |\mathbf{y}_\perp|^2 d\mathbf{y}_\perp \right) \right], \\ H_{33} &= \frac{2\pi^2}{\lambda_0^2 L^4} \left[\frac{1}{|D_a|} \int_{D_a} |\mathbf{y}_\perp|^4 d\mathbf{y}_\perp - \left(\frac{1}{|D_a|} \int_{D_a} |\mathbf{y}_\perp|^2 d\mathbf{y}_\perp \right)^2 \right]. \end{aligned}$$

The hotspot volume is defined as before as $V_c = \pi^{3/2}(\det \mathbf{H})^{-1/2}$. If, additionally, D_a is a disk with center at $(0, 0)$ and radius $a/2$ then \mathbf{H} is diagonal and we have

$$H_{jj} = \frac{\pi^2 a^2}{2\lambda_0^2 L^2}, \quad j = 1, 2, \quad H_{33} = \frac{\pi^2 a^4}{96\lambda_0^2 L^4}, \quad V_c = \frac{8\sqrt{6}\lambda_0^3 L^4}{\pi^3 a^4}.$$

The maximum of the functional over a domain Ω whose volume is much larger than the hotspot volume is given by (29) as before.

4.3. Migration-based detection test

The imaging functional in the presence of a reflector and noise is the superposition of a Gaussian random field with mean zero and covariance (28) and a peak centered at \mathbf{x}_{ref} with shape (25). We assume that the function $\mathcal{H}(\mathbf{x}, \mathbf{y})^2$ is of the form $h(\mathbf{x} - \mathbf{y})$, as in the case of the full or partial array described above. We can then define the hotspot volume V_c .

We consider the ratio of the maximum of the functional over its averaged value over the domain Ω :

$$S := \frac{\|\mathcal{I}_{\text{RT}}\|_{L^\infty(\Omega)}^2 |\Omega|}{\|\mathcal{I}_{\text{RT}}\|_{L^2(\Omega)}^2}. \quad (30)$$

In the regime in which $|\Omega|\delta^2 \leq V_c \sigma_{\text{ref}}^2$, the peak corresponding to the reflector is of the order of σ_{ref} , which is of the order of or larger than $\delta \sqrt{|\Omega|/V_c}$, which is much larger than $\delta \ln(|\Omega|/V_c)^{1/2}$. Therefore the peak is much stronger than the speckle in the imaging functional, and detection is trivial. In the following we address the non-trivial regime in which $|\Omega|\delta^2 \gg V_c \sigma_{\text{ref}}^2$. In this case, the L^2 -norm of the imaging functional $\|\mathcal{I}_{\text{RT}}\|_{L^2(\Omega)}^2$ is determined by the speckle and not by the peak due to the reflector and it is a self-averaging quantity given by $2\delta^2 |\Omega|$.

Proposition 4.1:

- a) If the response matrix is obtained in the absence of a reflector and $|\Omega| \gg V_c$, then

$$S \stackrel{\text{dist.}}{=} \ln \frac{|\Omega|}{V_c} + \frac{3}{2} \ln \ln \frac{|\Omega|}{V_c} - \ln Z_0, \quad (31)$$

where Z_0 follows an exponential distribution with mean one.

- b) If the response matrix is obtained in the presence of a reflector, $|\Omega| \gg V_c$, and

$\sigma_{\text{ref}} > \delta$, then

$$S \stackrel{\text{dist.}}{=} \max \left\{ \frac{\sigma_{\text{ref}}^2}{2\delta^2} + \frac{\sigma_{\text{ref}}}{\delta} Z, \ln \frac{|\Omega|}{V_c} + \frac{3}{2} \ln \ln \frac{|\Omega|}{V_c} - \ln Z_0 \right\}, \quad (32)$$

where Z_0 follows an exponential distribution with mean one and Z follows a Gaussian distribution with mean zero and variance one and are independent.

In (32) the first term in the maximum comes from the peak generated by the point reflector that is randomly perturbed by the noise (see (41) in Subsection 5.3), while the second term is the maximum of the speckle in the image.

If the data gives the ratio S , then we propose to use a test of the form $S > s$ for the alarm corresponding to the presence of a reflector. By the Neyman-Pearson lemma the decision rule of accepting H_A if and only if $S > s_\alpha$ maximizes the probability of detection (POD) for a given false alarm rate (FAR) α

$$\text{FAR} = \alpha = \mathbb{P}(S > s_\alpha | H_0),$$

with the threshold

$$s_\alpha = \ln \frac{|\Omega|}{V_c} + \frac{3}{2} \ln \ln \frac{|\Omega|}{V_c} + \Phi_G^{-1}(1 - \alpha), \quad (33)$$

where $\Phi_G(x) = \exp(-e^{-x})$ is the cumulative distribution function of the Gumbel distribution. The level s_α depends on α through a Gumbel table. We have, for instance, $\Phi_G^{-1}(0.9) \simeq 2.25$, $\Phi_G^{-1}(0.95) \simeq 2.97$, and $\Phi_G^{-1}(0.99) \simeq 4.60$. The level s_α also depends on the volume of the search domain Ω , that we know, and on the hotspot volume V_c , that we may not know. However, the estimation of V_c from the data is possible by computing the empirical cross correlation of the imaging functional \mathcal{I}_{RT} and fitting the peak at $\mathbf{0}$ with a quadratic form.

The probability of detection $1 - \beta$ is the probability to sound the alarm when there is a reflector:

$$\text{POD} = 1 - \beta = \mathbb{P}(S > s_\alpha | H_A).$$

It depends on the value σ_{ref} and on the noise level δ . Here we find that the probability of detection is

$$\text{POD} = 1 - \beta = \Phi \left(\frac{\frac{\sigma_{\text{ref}}^2}{2\delta^2} - s_\alpha}{\frac{\sigma_{\text{ref}}}{\delta}} \right),$$

where Φ is the cumulative distribution function of the normal distribution with mean zero and variance one. This result is valid as long as the first term in the right side of (32) is larger than the second term, which occurs when the POD becomes equal to α . Therefore we have

$$\text{POD} = \max \left\{ \Phi \left(\frac{1}{2} \frac{\sigma_{\text{ref}}}{\delta} - s_\alpha \frac{\delta}{\sigma_{\text{ref}}} \right), \alpha \right\}. \quad (34)$$

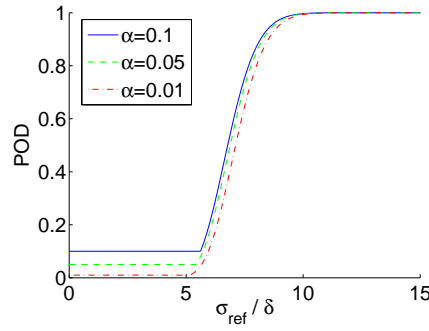


Figure 5. Probability of detection of the migration-based test as a function of $\sigma_{\text{ref}}/\delta$, for different false alarm rates α . Here $|\Omega|/V_c = 10^6$.

4.4. Discussion

To summarize, the migration-based test becomes powerful when $\sigma_{\text{ref}} > \sqrt{2}\delta \ln^{1/2}(|\Omega|/V_c)$. Remember that the SV-based test becomes powerful when $\sigma_{\text{ref}} > \delta\sqrt{n}$. Therefore the migration-based test is more (resp. less) powerful than the SV-based test when $n >$ (resp. $<$) $2 \ln(|\Omega|/V_c)$. In practice, we usually have $n > 2 \ln(|\Omega|/V_c)$, and therefore the migration-based test is more efficient than the SV-based test. We can interpret the difference between the two tests as follows. The SV-based test is essentially based on the maximization of $\bar{\mathbf{u}}^T \mathbf{A} \bar{\mathbf{u}}$ over all unit vectors \mathbf{u} (which gives the first singular value), while the migration-based test is essentially based on the maximization of $\bar{\mathbf{g}}^T \mathbf{A} \bar{\mathbf{g}}$ over all unit vectors \mathbf{g} of the form $\mathbf{g}(\mathbf{x})$ for some $\mathbf{x} \in \Omega$. The migration-based test uses the known structure of the singular vector associated to the reflector and is therefore more efficient than the SV-based test that does not exploit this information.

The SV-based test is simpler to implement than the migration-based test. On the one hand, the level r_α of the SV-based test (22) depends only on the number of sensors n . On the other hand, the level s_α of the migration-based test (33) depends also on the volume of the search domain Ω , that we know, and on the hotspot volume V_c , that we may not know. However, the estimation of V_c from the data is possible by computing the empirical cross correlation of the imaging functional \mathcal{I}_{RT} and fitting the peak at $\mathbf{0}$ with a quadratic form.

5. Optimal migration for localization

In this section we go further by considering the localization problem once we have detected the presence of a point reflector. We compare different imaging functionals for localizing a point reflector, in particular weighted-subspace migration functionals. We show the optimality of the reverse-time migration method in the presence of noise for localizing a point reflector.

5.1. Weighted-subspace migration

Let \mathbf{A} be the measured response matrix and $(\mathbf{v}^{(l)})_{l=1,\dots,n}$ form an orthonormal basis of the image space of \mathbf{A} :

$$\mathbf{A} = \sum_{l=1}^n \sigma^{(l)} \mathbf{v}^{(l)} (\mathbf{v}^{(l)})^T.$$

A general imaging functional can be obtained using a weighted-subspace migration [11]:

$$\begin{aligned}\mathcal{I}_{\text{SM}}(\mathbf{x}, \mathbf{w}) &:= \overline{\mathbf{g}(\mathbf{x})}^T \left[\sum_{l=1}^n w_l(\mathbf{x}) \mathbf{v}^{(l)} (\mathbf{v}^{(l)})^T \right] \overline{\mathbf{g}(\mathbf{x})} \\ &= \sum_{l=1}^n w_l(\mathbf{x}) (\overline{\mathbf{g}(\mathbf{x})}^T \mathbf{v}^{(l)})^2,\end{aligned}\quad (35)$$

where $\mathbf{w}(\mathbf{x}) = (w_l(\mathbf{x}))_{l=1, \dots, n}$ are filter (complex) weights that can depend on the singular values and on the singular vectors of the measured MSR matrix and $\mathbf{g}(\mathbf{x})$ is the normalized vector of Green's functions (6).

Consider in particular the weights:

$$w_l^{(1)}(\mathbf{x}) := \sigma^{(l)}, \quad w_l^{(2)}(\mathbf{x}) := \exp\left(-i2 \arg\left(\overline{\mathbf{g}(\mathbf{x})}^T \mathbf{v}^{(1)}\right)\right) \mathbf{1}_1(l).$$

Then $\mathcal{I}_{\text{SM}}(\mathbf{x}, \mathbf{w}^{(1)})$ corresponds to reverse-time migration (24):

$$\mathcal{I}_{\text{SM}}(\mathbf{x}, \mathbf{w}^{(1)}) = \mathcal{I}_{\text{RT}}(\mathbf{x}). \quad (36)$$

Moreover we have the following connection of $\mathcal{I}_{\text{SM}}(\mathbf{x}, \mathbf{w}^{(2)})$ to the MUSIC algorithm:

$$\begin{aligned}\mathcal{I}_{\text{MUSIC}}(\mathbf{x}) &:= \left\| \mathbf{g}(\mathbf{x}) - (\overline{\mathbf{v}^{(1)}}^T \mathbf{g}(\mathbf{x})) \mathbf{v}^{(1)} \right\|^{-1/2} = \left(1 - \left| \overline{\mathbf{g}(\mathbf{x})}^T \mathbf{v}^{(1)} \right|^2\right)^{-1/2} \\ &= \left(1 - \mathcal{I}_{\text{SM}}(\mathbf{x}, \mathbf{w}^{(2)})\right)^{-1/2}.\end{aligned}\quad (37)$$

The next subsection will make it clear that an appropriate weighted-subspace migration is optimal to find the location of the reflector in the presence of noise.

5.2. Optimal migration functional

The main result of this section is the following proposition.

Proposition 5.1: *Given the response matrix \mathbf{A} , the estimator*

$$\hat{\mathbf{x}} = \operatorname{argmax}_{\mathbf{x} \in \Omega} |\mathcal{I}_{\text{RT}}(\mathbf{x})|^2 \quad (38)$$

is the best estimator (in the maximum likelihood sense) to localize a reflector buried in the search domain Ω .

This result holds in the presence of additive noise. The estimator (38) may be not optimal for more complex cluttered noise for instance.

This proposition shows that the weighted-subspace migration with the weights $\mathbf{w}^{(1)}$, corresponding to reverse-time imaging, is more appropriate for the localization of the reflector than the weighted-subspace migration \mathcal{I}_{SM} with the weights $\mathbf{w}^{(2)}$, corresponding to MUSIC, or even to the Kirchhoff migration functional:

$$\mathcal{I}_{\text{KM}}(\mathbf{x}) := \overline{\mathbf{d}(\mathbf{x})}^T \mathbf{A} \overline{\mathbf{d}(\mathbf{x})},$$

which is close to the reverse-time imaging functional, but in which the amplitude of the Green function for the backpropagation is normalized:

$$\mathbf{d}(\mathbf{x}) := \frac{1}{\sqrt{n}} \left(\exp(i\frac{\omega}{c_0}|\mathbf{x} - \mathbf{x}_j|) \right)_{j=1, \dots, n}.$$

Proof. We assume the model (11) for the data \mathbf{A} . Given the observations \mathbf{A} , we find by using Bayes theorem with the Jeffreys prior for the parameters (a non-informative prior distribution) that the likelihood function of the parameters \mathbf{x} (the reflector location), σ (the reflector singular value), and δ^2 (the noise variance) is proportional to

$$l_0(\mathbf{x}, \sigma, \delta^2 | \mathbf{A}) = \frac{1}{\delta^{n^2+n+1}} \exp \left(- \frac{\|\mathbf{A} - \sigma \mathbf{g}(\mathbf{x}) \mathbf{g}(\mathbf{x})^T\|_F^2}{2\delta^2} \right), \quad (39)$$

with the subscript F representing Frobenius norm. The maximum likelihood estimate of \mathbf{x} and the nuisance parameters δ^2 and σ are found by maximizing the likelihood function (39) with respect to these:

$$(\hat{\mathbf{x}}, \hat{\sigma}, \hat{\delta}^2) = \underset{\mathbf{x}, \sigma, \delta^2}{\operatorname{argmax}} l_0(\mathbf{x}, \sigma, \delta^2 | \mathbf{A}).$$

We first eliminate δ^2 by requiring

$$\frac{\partial l_0(\mathbf{x}, \sigma, \delta^2 | \mathbf{A})}{\partial \delta} = 0.$$

This gives

$$\hat{\delta}^2 = \frac{\|\mathbf{A} - \sigma \mathbf{g}(\mathbf{x}) \mathbf{g}(\mathbf{x})^T\|_F^2}{n^2 + n + 1},$$

and the likelihood ratio is then proportional to

$$l_0(\mathbf{x}, \sigma, \hat{\delta}^2 | \mathbf{A}) \simeq \|\mathbf{A} - \sigma \mathbf{g}(\mathbf{x}) \mathbf{g}(\mathbf{x})^T\|_F^{-(n^2+n+1)/2}.$$

Note that we have

$$\|\mathbf{A} - \sigma \mathbf{g}(\mathbf{x}) \mathbf{g}(\mathbf{x})^T\|_F^2 = \|\tilde{\mathbf{v}} - \sigma \tilde{\mathbf{g}}(\mathbf{x})\|_2^2$$

for $\tilde{\mathbf{v}} = \sum_{l=1}^n \sigma^{(l)} \mathbf{v}^{(l)} \otimes \mathbf{v}^{(l)}$ and $\tilde{\mathbf{g}}(\mathbf{x}) = \mathbf{g}(\mathbf{x}) \otimes \mathbf{g}(\mathbf{x})$. Using that $\|\tilde{\mathbf{g}}(\mathbf{x})\|_2 = \|\mathbf{g}(\mathbf{x})\|^2 = 1$, we find

$$\hat{\sigma} = \underset{\sigma}{\operatorname{argmin}} \|\tilde{\mathbf{v}} - \sigma \tilde{\mathbf{g}}(\mathbf{x})\|_2^2 = \overline{\tilde{\mathbf{g}}(\mathbf{x})}^T \tilde{\mathbf{v}}.$$

We therefore conclude that the estimate $\hat{\mathbf{x}}$ of the reflector location derives from

$$\hat{\mathbf{x}} = \underset{\mathbf{x}}{\operatorname{argmin}} \left\| \tilde{\mathbf{v}} - \left(\overline{\tilde{\mathbf{g}}(\mathbf{x})}^T \tilde{\mathbf{v}} \right) \tilde{\mathbf{g}}(\mathbf{x}) \right\|_2^2.$$

Note that

$$\left\| \tilde{\mathbf{v}} - \left(\overline{\tilde{\mathbf{g}}(\mathbf{x})}^T \tilde{\mathbf{v}} \right) \tilde{\mathbf{g}}(\mathbf{x}) \right\|_2^2 = \|\tilde{\mathbf{v}}\|_2^2 - \left| \overline{\tilde{\mathbf{g}}(\mathbf{x})}^T \tilde{\mathbf{v}} \right|^2 = \|\tilde{\mathbf{v}}\|_2^2 - \left| \sum_{l=1}^n \sigma^{(l)} \left(\overline{\mathbf{g}(\mathbf{x})}^T \mathbf{v}^{(l)} \right)^2 \right|^2.$$

From this representation we find that the estimate of the reflector location can be expressed in terms of the weighted-subspace migration \mathcal{I}_{SM} with the weights $\mathbf{w}^{(1)} = (\sigma^{(l)})_{l=1, \dots, n}$, which is the reverse-time imaging functional \mathcal{I}_{RT} defined by (36): This gives $\hat{\mathbf{x}} = \underset{\mathbf{x}}{\operatorname{argmin}} (\|\tilde{\mathbf{v}}\|_2^2 - |\mathcal{I}_{\text{RT}}(\mathbf{x})|^2)$, which completes the proof of the proposition. \square

5.3. Statistical analysis of the localization error

The localization of the reflector consists in looking after the maximum of an imaging functional. In the presence of a reflector at \mathbf{x}_{ref} the imaging functional has the form

$$\mathcal{I}_{\text{RT}}(\mathbf{x}) = \sigma_{\text{ref}} h(\mathbf{x} - \mathbf{x}_{\text{ref}}) + \mathcal{I}_1(\mathbf{x}),$$

where \mathcal{I}_1 is a complex Gaussian random field with mean zero, variance $2\delta^2$ and smooth covariance function $2\delta^2 h(\mathbf{x} - \mathbf{y})$.

We consider the case in which h is real-valued. The case in which h is complex-valued can be addressed by introducing an auxiliary field as in Subsection 4.2. A Taylor series expansion around \mathbf{x}_{ref} gives:

$$|\mathcal{I}_{\text{RT}}(\mathbf{x})|^2 \simeq \left| \sigma_{\text{ref}} \left(1 - \frac{1}{2} (\mathbf{x} - \mathbf{x}_{\text{ref}})^T \mathbf{H} (\mathbf{x} - \mathbf{x}_{\text{ref}}) \right) + \mathcal{I}_1(\mathbf{x}_{\text{ref}}) + \nabla \mathcal{I}_1(\mathbf{x}_{\text{ref}})^T (\mathbf{x} - \mathbf{x}_{\text{ref}}) \right|^2,$$

so that the estimation of the location of the maximum has the form:

$$\hat{\mathbf{x}} = \underset{\mathbf{x}}{\operatorname{argmax}} |\mathcal{I}_{\text{RT}}(\mathbf{x})|^2 = \mathbf{x}_{\text{ref}} + \frac{1}{\sigma_{\text{ref}}} \operatorname{Re}(\mathbf{H}^{-1} \nabla \mathcal{I}_1(\mathbf{x}_{\text{ref}})),$$

provided the error is not too large (smaller than the radius of a hotspot). To leading order (in $\delta/\sigma_{\text{ref}}$) the estimation $\hat{\mathbf{x}}$ is unbiased, i.e. its mean is the true location \mathbf{x}_{ref} . Moreover, using the fact that $\mathbb{E}[\operatorname{Re} \nabla \mathcal{I}_1(\mathbf{x}_{\text{ref}}) \operatorname{Re} \nabla \mathcal{I}_1(\mathbf{x}_{\text{ref}})^T] = \delta^2 \mathbf{H}$, the covariance matrix of the estimator $\hat{\mathbf{x}}$ is

$$\mathbb{E}[(\hat{\mathbf{x}} - \mathbf{x}_{\text{ref}})(\hat{\mathbf{x}} - \mathbf{x}_{\text{ref}})^T] = \frac{\delta^2}{\sigma_{\text{ref}}^2} \mathbf{H}^{-1}. \quad (40)$$

This means that the relative error (relative to the radius of the peak function h) in the localization of the reflector is of the order of $\delta/\sigma_{\text{ref}}$. Note also that, as a byproduct of this analysis, we find that the perturbed value of the maximum of the peak is of the form

$$|\mathcal{I}_{\text{RT}}(\hat{\mathbf{x}})|^2 \simeq \sigma_{\text{ref}}^2 + 2\sigma_{\text{ref}} \operatorname{Re}(\mathcal{I}_1(\mathbf{x}_{\text{ref}})) + O(\delta^2), \quad (41)$$

where $\operatorname{Re}(\mathcal{I}_1(\mathbf{x}_{\text{ref}}))$ follows a Gaussian distribution with mean 0 and variance δ^2 .

Full aperture array. If the medium is homogeneous and three-dimensional, if the sensor array is dense and surrounds the region of interest, then we have

$$\mathbb{E}[(\hat{x}_j - x_{\text{ref},j})^2] = \frac{\delta^2}{\sigma_{\text{ref}}^2} \frac{3\lambda_0^2}{8\pi^2}, \quad j = 1, \dots, 3.$$

Finite aperture array. If the medium is homogeneous and three-dimensional, if the sensor array is dense and occupies the domain $D_a \times \{0\}$, with D_a the disk in \mathbb{R}^2 centered at $(0,0)$ with diameter a , and the search region is a domain Ω around $(0,0,L)$ with $L \gg a$, then we have in the transverse directions and in the longitudinal direction

$$\mathbb{E}[(\hat{x}_j - x_{\text{ref},j})^2] = \frac{\delta^2}{\sigma_{\text{ref}}^2} \frac{2\lambda_0^2 L^2}{\pi^2 a^2}, \quad j = 1, 2, \quad \mathbb{E}[(\hat{x}_3 - x_{\text{ref},3})^2] = \frac{\delta^2}{\sigma_{\text{ref}}^2} \frac{96\lambda_0^2 L^4}{\pi^2 a^4}.$$

5.4. Numerical simulations

The configuration for the numerical experiment is the following one:

- $n = 100$ sensors with location $(x_j, 0, 0)$ with $x_j = -200 + 4j$, $j = 0, \dots, 100$.
 - one point reflector with location $\mathbf{x}_{\text{ref}} = (0, 0, 50)$, with reflectivity $\sigma_{\text{ref}} l_{\text{ref}}^3 = 0.018$.
- Since $\lambda_0 = 1$, $c_0 = 1$, this gives $\sigma_{\text{ref}} \simeq 5.9 \cdot 10^{-5}$ from (8).

In Figure 6 the unperturbed imaging functionals are plotted in the (x, z) -plane (the MUSIC functional is in fact the weighted-subspace migration functional (35) with the weight $\mathbf{w}^{(2)}$).

In Figure 7 the imaging functionals are plotted in the presence of noise with $\delta = 6 \cdot 10^{-6}$, which corresponds to $\sigma_c = 6 \cdot 10^{-5}$. It is possible to see that the MUSIC functional can be completely wrong, because the selected singular vector (i.e., the one corresponding to the largest singular value) used for the backpropagation is not correct (i.e., it is not the one associated to the reflector).

In Figure 8 the standard deviation in the reflector location is plotted versus the noise level for the different imaging functionals. As predicted by the theory the MUSIC algorithm is not very robust and fails when $\delta > 5 \cdot 10^{-6}$, or equivalently $\sigma_c > 5 \cdot 10^{-5} \sim \sigma_{\text{ref}}$. The reverse-time imaging functional is more robust, and for moderate noise level the standard deviation is linear in δ . Indeed the reverse-time imaging functional backpropagates not only the first singular vector, but all of them (weighted by their singular values), and since only the backpropagation of the singular vector corresponding to the reflector gives a peak, while the backpropagation of the other singular vectors just gives noise, we can still observe a peak centered at the reflector location even in the regime when the first singular vector is not the one corresponding to the reflector. This is what is shown by the statistical arguments developed in the previous section.

We can also notice that reverse-time imaging performs slightly better than Kirchhoff migration imaging. This is in agreement with the theory of the previous section and can be noticed in the simulations carried out here because the array has very large aperture, so that the amplitudes of the Green functions in the vector $\mathbf{g}(\mathbf{x})$ are not constant. If the array has small aperture then the vectors $\mathbf{g}(\mathbf{x})$ (used in reverse-time migration) and $\mathbf{d}(\mathbf{x})$ (used in Kirchhoff migration) are very similar and the difference between the two imaging functionals is small.

6. Conclusion

In this paper we have carefully studied detection tests based on the singular values of the response matrix on the one hand and on weighted-subspace migration functionals on the other hand, by using recent tools of random matrix theory and extreme value theory. In both cases we have proved a form of optimality in that the tests are the most powerful for a given false alarm rate in the presence of additive noise. We have proved that the migration-based test is more powerful than the

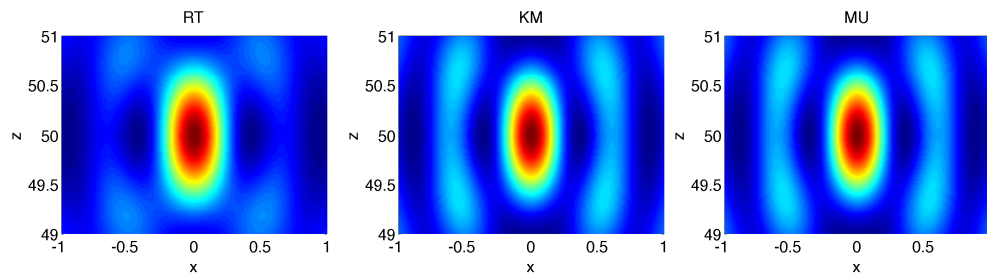


Figure 6. Imaging functionals in the absence of noise (left: reverse-time migration, center: Kirchhoff migration, right: MUSIC).

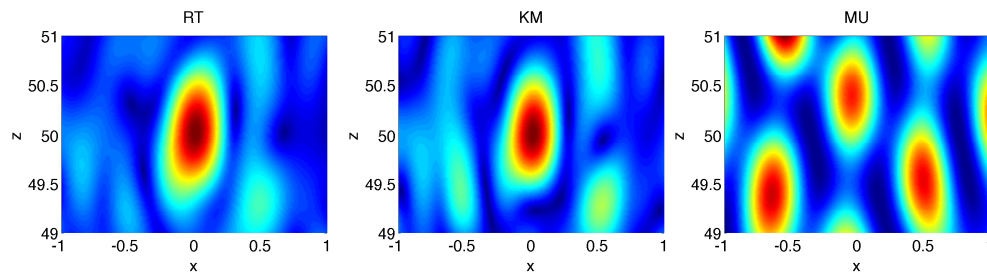


Figure 7. Imaging functionals in the presence of noise.

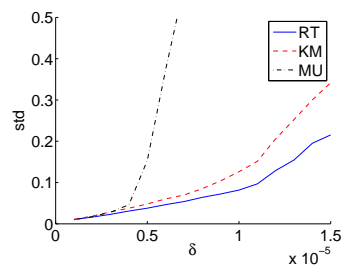


Figure 8. Standard deviation of the estimated reflector location obtained with three different migration methods.

SV-based test and we explain this result by remarking that the migration-based exploits the structure of the reflector singular vector, while the SV-based test does not use it. We have also proved that, once the detection test comes out positive, reflector localization should be performed with reverse-time migration rather than any other form of weighted-subspace migration.

In this paper we have assumed that the background medium is homogeneous for simplicity. It is possible to extend the results to the case in which the medium is slowly and smoothly varying. We would obtain the same results as the one derived in this paper by using a geometric approximation for the Green function associated with the inhomogeneous medium.

The case with a point reflector that we address in this paper is a very simple model, but the results could be extended to the detection and localization of small inclusions and cracks using the asymptotic formalism provided in [3, 4]. This is because results on low-rank perturbations of random Gaussian matrices are available and could be used as we did here [13, 14, 17].

Appendix A. The Born approximation for a point reflector

We briefly describe the Born approximation [12] for the point reflector introduced in Section 2.2 to calculate the response in the presence of a reflector. We assume that the medium is homogeneous with background velocity c_0 and that the localized reflector around \mathbf{x}_{ref} is modeled by the local variation $V_{\text{ref}}(\mathbf{x})$ of the speed of propagation defined via (2). The solution of the full time-harmonic wave equation (3) can be written as the sum

$$\hat{u}(\omega, \mathbf{x}, \mathbf{y}) = \hat{G}_0(\omega, \mathbf{x}, \mathbf{y}) + \hat{u}_1(\omega, \mathbf{x}, \mathbf{y}),$$

where \hat{G}_0 is the time-harmonic Green function of the background medium. The scattered field \hat{u}_1 is solution of the homogeneous wave equation with the source term $\omega^2 c_0^{-2} \sigma_r V_{\text{ref}}(\mathbf{x}) \hat{u}(\omega, \mathbf{x}, \mathbf{y})$, so that it is given by

$$\hat{u}_1(\omega, \mathbf{x}, \mathbf{y}) = \frac{\omega^2}{c_0^2} \int \hat{G}_0(\omega, \mathbf{x}, \mathbf{z}) \sigma_r V_{\text{ref}}(\mathbf{z}) \hat{u}(\omega, \mathbf{z}, \mathbf{y}) d\mathbf{z}. \quad (\text{A1})$$

This expression is exact. The Born approximation (or single-scattering approximation) consists in replacing \hat{u} on the right side of (A1) by the field \hat{G}_0 , which gives:

$$\hat{u}_1(\omega, \mathbf{x}, \mathbf{y}) \simeq \frac{\omega^2}{c_0^2} \int \hat{G}_0(\omega, \mathbf{x}, \mathbf{z}) \sigma_r V_{\text{ref}}(\mathbf{z}) \hat{G}_0(\omega, \mathbf{z}, \mathbf{y}) d\mathbf{z}.$$

This approximation is valid if the scattered field \hat{u}_1 is small compared to the incident field \hat{G}_0 , which holds if the scattering amplitude σ_r is small. We also assume that the diameter l_{ref} of the scattering region Ω_{ref} is small compared to typical wavelength. We can then model the scatterer by a point scatterer and we can write the scattered field \hat{u}_1 in the form

$$\hat{u}_1(\omega, \mathbf{x}, \mathbf{y}) = \frac{\omega^2}{c_0^2} \sigma_r l_{\text{ref}}^3 \hat{G}_0(\omega, \mathbf{x}, \mathbf{x}_{\text{ref}}) \hat{G}_0(\omega, \mathbf{x}_{\text{ref}}, \mathbf{y}). \quad (\text{A2})$$

Appendix B. Some results on complex Gaussian random fields

Let $\Omega \subset \mathbb{R}^d$ be a bounded domain and let $(A(\mathbf{x}))_{\mathbf{x} \in \Omega}$ be a stationary complex Gaussian random field with mean zero, i.e. a speckle pattern. The statistical distribution of the random field is characterized by the covariance function:

$$C(\mathbf{x}) := \mathbb{E}[\overline{A(\mathbf{x}')} A(\mathbf{x}' + \mathbf{x})].$$

We assume here that C is real-valued and smooth, so that the realizations of the random field are smooth [1, Theorem 1.4.2]. As we will see below, the relevant statistical information about local and global maxima of the field is in the mean intensity $I_0 = C(\mathbf{0}) = \mathbb{E}[|A(\mathbf{x})|^2]$ and in the matrix

$$\mathbf{\Lambda} := \left(\mathbb{E}[\overline{\partial_{x_j} A(\mathbf{x})} \partial_{x_l} A(\mathbf{x})] \right)_{j,l=1,\dots,d} = \left(-\partial_{x_j x_l}^2 C(\mathbf{0}) \right)_{j,l=1,\dots,d}.$$

B.1. Local maxima of a complex Gaussian random field

We consider the intensity profile of the complex field:

$$I(\mathbf{x}) := |A(\mathbf{x})|^2,$$

and we look for the statistical distribution of the local maxima of $I(\mathbf{x})$.

Let us denote by M_u^Ω the number of local maxima of $I(\mathbf{x})$ in Ω with values larger than u :

$$M_u^\Omega := \text{Card}\{ \text{local maxima of } (I(\mathbf{x}))_{\mathbf{x} \in \Omega} \text{ with values larger than } u \}.$$

We have [26, Theorem 3.3]

$$\mathbb{E}[M_u^\Omega] = \frac{|\Omega|}{V_c} \left(\frac{u}{I_0}\right)^{\frac{d}{2}} \exp\left(-\frac{u}{I_0}\right) \left(1 + O\left(\left(\frac{u}{I_0}\right)^{-1/2}\right)\right), \text{ for } u \gg I_0,$$

where V_c is the hotspot volume defined in terms of the determinant of the Hessian of the covariance function as:

$$V_c := \frac{I_0^{d/2} \pi^{d/2}}{(\det \mathbf{\Lambda})^{1/2}}.$$

B.2. Global maximum of a complex Gaussian random field

Let us denote by I_{\max}^Ω the global maximum of the field over the domain Ω :

$$I_{\max}^\Omega := \max_{\mathbf{x} \in \Omega} |A(\mathbf{x})|^2.$$

Using [26, Corollary 3.4] it is possible to show that, when $|\Omega| \gg V_c$, the statistical distribution of I_{\max}^Ω is of the form

$$I_{\max}^\Omega = I_0 \left[\ln\left(\frac{|\Omega|}{V_c}\right) + \frac{d}{2} \ln \ln\left(\frac{|\Omega|}{V_c}\right) - \ln Z_0 \right],$$

where Z_0 follows an exponential distribution, or equivalently $-\ln Z_0$ follows a Gumbel distribution with cumulative distribution function $\mathbb{P}(-\ln Z_0 \leq x) = \exp(-e^{-x})$.

B.3. The local shape of a local maximum

We first state a classical and fundamental lemma about Gaussian vectors.

Let us consider a $\mathbb{R}^{n_1+n_2}$ -valued random vector $\begin{pmatrix} \mathbf{y}_1 \\ \mathbf{y}_2 \end{pmatrix}$ with Gaussian statistics:

$$\mathcal{L}\left(\begin{pmatrix} \mathbf{y}_1 \\ \mathbf{y}_2 \end{pmatrix}\right) \sim \mathcal{N}\left(\begin{pmatrix} \bar{\mathbf{y}}_1 \\ \bar{\mathbf{y}}_2 \end{pmatrix}, \begin{pmatrix} \mathbf{R}_{11} & \mathbf{R}_{12} \\ \mathbf{R}_{21} & \mathbf{R}_{22} \end{pmatrix}\right).$$

The mean vectors $\bar{\mathbf{y}}_1$ and $\bar{\mathbf{y}}_2$ are in \mathbb{R}^{n_1} and \mathbb{R}^{n_2} , respectively, the covariance matrix \mathbf{R}_{11} has size $n_1 \times n_1$, \mathbf{R}_{12} has size $n_1 \times n_2$, $\mathbf{R}_{21} = \mathbf{R}_{12}^T$ has size $n_2 \times n_1$, and \mathbf{R}_{22} has size $n_2 \times n_2$. Assume that the distribution of \mathbf{y}_2 is not degenerate, i.e., that

\mathbf{R}_{22} is invertible.

Then, conditioned on \mathbf{y}_2 , the distribution of \mathbf{y}_1 is Gaussian:

$$\mathcal{L}(\mathbf{y}_1|\mathbf{y}_2) \sim \mathcal{N}\left(\bar{\mathbf{y}}_1 + \mathbf{R}_{12}\mathbf{R}_{22}^{-1}(\mathbf{y}_2 - \bar{\mathbf{y}}_2), \mathbf{R}_{11} - \mathbf{R}_{12}\mathbf{R}_{22}^{-1}\mathbf{R}_{21}\right).$$

Using this lemma one can show that, given that the random field $A(\mathbf{x})$ has a local maximum at \mathbf{x}_0 with amplitude A_0 (with $|A_0| \gg \sqrt{I_0}$), then we have locally around \mathbf{x}_0 :

$$A(\mathbf{x}) \simeq A_0 \left[\frac{C(\mathbf{x} - \mathbf{x}_0)}{I_0} + o(1) \right], \quad [|A_0| \gg \sqrt{I_0}].$$

References

- [1] R. Adler and J. Taylor, *Random Fields and Geometry*, Springer, New York, 2007.
- [2] E. Akkermans and G. Montambaux, Coherent multiple scattering in disordered media, in *Waves and Imaging through Complex Media*, P. Sebbah, ed., Kluwer, Dordrecht, 2001, pp. 29–52 (cond-mat/0104013).
- [3] H. Ammari and H. Kang, *Reconstruction of Small Inhomogeneities from Boundary Measurements*, Lecture Notes in Mathematics, Vol. 1846, Springer-Verlag, Berlin, 2004.
- [4] H. Ammari, H. Kang, H. Lee, and W.K. Park, Asymptotic imaging of perfectly conducting cracks, *SIAM J. Sci. Comput.* **32** (2010), 894–922.
- [5] A. Aubry and A. Derode, Random matrix theory applied to acoustic backscattering and imaging in complex media, *Phys. Rev. Lett.* **102** (2009), 084301.
- [6] A. Aubry and A. Derode, Singular value distribution of the propagation matrix in random scattering media, *Waves Random Complex Media* (2010), in press (arXiv:0904.0161v2).
- [7] A. Aubry and A. Derode, Detection and imaging in a random medium: A matrix method to overcome multiple scattering and aberration, *J. Appl. Physics* **106** (2009), 044903.
- [8] J. Bayk, R. Buckingham, and J. DiFranco, Asymptotics of Tarcy-Widom distributions and the total integral of a Painlevé II function, *Comm. Math. Phys.* **280** (2008), 463–397.
- [9] N. Bleistein, J. Cohen, and J. S. Jr Stockwell, *Mathematics of Multidimensional Seismic Imaging, Migration, and Inversion*, Springer, New York, 2001.
- [10] L. Borcea, G. Papanicolaou, C. Tsogka, and J. Berryman, Imaging and time reversal in random media, *Inverse Problems* **18** (2002) 1247–1279.
- [11] L. Borcea, G. Papanicolaou, and F. G. Vasquez, Edge illumination and imaging of extended reflectors, *SIAM J. Imaging Sci.* **1** (2008), 75–114.
- [12] M. Born and E. Wolf, *Principles of Optics*, Academic Press, New York, 1970.
- [13] M. Capitaine, C. Donati-Martin, and D. Féral, The largest eigenvalue of finite rank deformation of large Wigner matrices: convergence and nonuniversality of the fluctuations, *Ann. Probab.* **37** (2009), 1–47.
- [14] M. Capitaine, C. Donati-Martin, and D. Féral, Central limit theorems for eigenvalues of deformations of Wigner matrices, arXiv:0903.4740v1.
- [15] G. Casella and R. L. Berger, *Statistical Inference*, Duxbury Press, Pacific Grove, 2002.
- [16] A. J. Devaney, Time reversal imaging of obscured targets from multistatic data, *IEEE Trans. Antennas Propagat.* **523** (2005), 1600–1610.
- [17] D. Féral and S. Péché, The largest eigenvalue of rank one deformation of large Wigner matrices, *Comm. Math. Phys.* **272** (2007), 185–228.
- [18] A. Gut, *Probability: A Graduate Course*, Springer-Verlag, New-York, 2005.
- [19] H. Lev-Ari and A. J. Devaney, The time-reversal technique reinterpreted: subspace based signal processing for multi-static target location, *EEE Sensor Array and Multichannel Signal Processing Workshop*, Cambridge, MA, March 2000, 509–513.
- [20] M. L. Mehta, *Random Matrices*, Academic Press, San Diego, 1991.
- [21] L. Pastur, On the spectrum of random matrices, *Teor. Math. Phys.* **10** (1972), 67–74.
- [22] S. Péché, The largest eigenvalue of small rank perturbations of Hermitian random matrices, *Probab. Theory Related Fields* **134** (2006), 127–173.
- [23] S. M. Popoff, G. Lerosey, R. Carminati, M. Fink, A. C. Boccara, and S. Gigan, Measuring the transmission matrix in optics: An approach to the study and control of light propagation in disordered media, *Phys. Rev. Lett.* **104** (2010), 100601.
- [24] C. Prada, S. Manneville, D. Spolianski, and M. Fink, Decomposition of the time reversal operator: detection and selective focusing on two scatterers, *J. Acoust. Soc. Am.* **99** (1996), 2067–2076.
- [25] R. A. DeVore and G. Lorentz, *Constructive Approximation*, Springer-Verlag, Berlin, 1993.
- [26] K. J. Worsley, Local maxima and the expected Euler characteristic of excursion sets of χ^2 , F , and t fields, *Adv. in Appl. Probab.* **26** (1994), 13–42.